Published OnlineFirst October 28, 2013; DOI: 10.1158/0008-5472.CAN-13-1103

MET and AXL Inhibitor NPS-1034 Exerts Efficacy against Lung Cancer Cells Resistant to EGFR Kinase Inhibitors Because of MET or AXL Activation

Jin Kyung Rho[1,2], Yun Jung Choi[1], Seon Ye Kim[1], Tae Won Kim[3], Eun Kyung Choi[4], Seon-Joo Yoon[5], Bu Man Park[5], Eunhye Park[5], Jong Hwan Bae[5], Chang-Min Choi[1,3], and Jae Cheol Lee[3]

Abstract

In non–small cell lung cancer (NSCLC) with epidermal growth factor receptor (EGFR) mutations, acquired resistance to EGFR-tyrosine kinase inhibitors (EGFR-TKI) can occur through a generation of bypass signals such as MET or AXL activation. In this study, we investigated the antitumor activity of NPS-1034, a newly developed drug that targets both MET and AXL, in NSCLC cells with acquired resistance to gefitinib or erlotinib (HCC827/GR and HCC827/ER, respectively). Characterization of H820 cells and evaluation of NPS-1034 efficacy in these cells were also performed. The resistance of HCC827/GR was mediated by MET activation, whereas AXL activation led to resistance in HCC827/ER. The combination of gefitinib or erlotinib with NPS-1034 synergistically inhibited cell proliferation and induced cell death in both resistant cell lines. Accordingly, suppression of Akt was noted only in the presence of treatment with both drugs. NPS-1034 was also effective in xenograft mouse models of HCC827/GR. Although the H820 cell line was reported previously to have T790M and MET amplification, we discovered that AXL was also activated in this cell line. There were no antitumor effects of siRNA or inhibitors specific for EGFR or MET, whereas combined treatment with AXL siRNA or NPS-1034 and EGFR-TKIs controlled H820 cells, suggesting that AXL is the main signal responsible for resistance. In addition, NPS-1034 inhibited cell proliferation as well as ROS1 activity in HCC78 cells with ROS1 rearrangement. Our results establish the efficacy of NPS-1034 in NSCLC cells rendered resistant to EGFR-TKIs because of MET or AXL activation or ROS1 rearrangement. *Cancer Res; 74(1); 253–62. ©2013 AACR.*

Introduction

The efficacy of epidermal growth factor receptor-tyrosine kinase inhibitors (EGFR-TKI), such as gefitinib and erlotinib, in non–small cell lung cancer (NSCLC) therapy has been demonstrated (1, 2). Their clinical benefits are clearly observed, especially in patients with *EGFR* mutations, such as G719A on exon 18, a deletion mutation on exon 19 and L858R on exon 21 (3, 4). The remarkable response of cancer cells with *EGFR* mutations to EGFR-TKIs may be explained by their dependency on EGFR signaling for growth and survival, the so-called "oncogene addiction" (5–7). However, despite an excellent initial response, drug resistance eventually develops in the majority of patients, limiting the mean drug–response duration to less than 1 year (8, 9).

Several resistance mechanisms, including the secondary T790M mutation and *MET* amplification, have been identified to date. The T790M mutation induces conformational changes in the ATP-binding pocket of EGFR, leading to reduced affinity for small molecule tyrosine kinase inhibitors or enhanced ATP binding affinity in oncogenic-mutated *EGFR* (10). *MET* amplification contributes to the acquisition of resistance to EGFR-TKIs (11) because it is a redundant pathway for the activation of PI3K/Akt signaling that facilitates the survival of cancer cells, thus by-passing the inhibition of upstream EGFR signaling in the presence of EGFR-TKIs. Interestingly, both mechanisms have been observed simultaneously in some patients. Clinical studies have disclosed that the T790M *EGFR* mutation is responsible for EGFR-TKI resistance in about 50% patients, whereas *MET* amplification is involved in an additional 5% of patients (8, 11–13).

AXL belongs to the TAM (Tyro-Axl-Mer) receptor tyrosine kinase (RTK) family and is characterized by 2 immunoglobulin-like domains, dual fibronectin type II repeats in the extracellular domain. Its ligands are vitamin K–dependent proteins, such as growth arrest-specific 6 (Gas6) and protein S (14). TAM signaling is related to cell survival, proliferation, migration, and phagocytosis (15–17) and may affect the downstream PI3K/

Authors' Affiliations: [1]Department of Pulmonology and Critical Care Medicine; [2]Asan Institute for Life Sciences; Departments of [3]Oncology and [4]Radiation Oncology, Asan Medical Center, College of Medicine, University of Ulsan, Songpa-gu, Seoul; and [5]Department of New Drug Discovery, Neopharm, Daejeon, South Korea

Note: Supplementary data for this article are available at Cancer Research Online (http://cancerres.aacrjournals.org/).

J. K. Rho and Y.J. Choi contributed equally to this work.

Corresponding Author: Jae Cheol Lee, Department of Oncology, Asan Medical Center, College of Medicine, University of Ulsan, 86 Asanbyeongwon-gil, Songpa-gu, Seoul 138-736, South Korea. Phone: 82-2-3010-3208; Fax: 82-2-3010-5956; E-mail: jclee@amc.seoul.kr

doi: 10.1158/0008-5472.CAN-13-1103

Published OnlineFirst October 28, 2013; DOI: 10.1158/0008-5472.CAN-13-1103

Akt and Janus kinase–STAT signaling pathways (18, 19). Recently, AXL has been a focus of research in the field of targeted therapy after its identification as a "tyrosine kinase switch" that induces resistance (20–22). We showed previously that AXL contributes to the survival of *EGFR*-mutant lung cancer cells in a manner similar to that observed for MET (23). Increased AXL expression was found in approximately 20% of patients with acquired resistance to EGFR-TKIs, as assessed by comparison of pre- and post-TKI tumor samples.

In this context, we expect that a drug targeting both MET and AXL would be very useful in patients with acquired resistance to EGFR-TKIs not caused by T790M. This study aimed to assess the efficacy of NPS-1034, a newly developed synthetic MET and AXL inhibitor, in NSCLC cells with resistance to EGFR-TKIs via the bypass signals of MET or AXL.

Materials and Methods

Cell culture and reagents

The human NSCLC cell lines HCC827 and H820 were obtained from the American Type Culture Collection (Rockville). Cells were cultured in RPMI 1640 medium containing 10% FBS, 2 mmol/L L-glutamine, and 100 units/mL of penicillin and streptomycin, and maintained at 37°C in a humidified chamber containing 5% CO_2. Erlotinib, gefitinib, and PHA-665752 were purchased from Selleck Chemicals.

Establishment of gefitinib- and erlotinib-resistant cell lines

Erlotinib-resistant cell lines were established in a previous study (23). Gefitinib-resistant variants of HCC827 were isolated by exposure to stepwise increasing doses of gefitinib. Briefly, HCC827 cells were treated with 10 nmol/L (the approximate IC_{50} dose) gefitinib for 72 hours in RPMI 1650 medium containing 10% FBS. Subsequently, cells were cultured in drug-free medium until 80% confluence. Cells were continuously exposed to increasing drug doses up to 1 μmol/L more than 8 months. The established resistant cell lines were maintained in medium containing 1 μmol/L gefitinib. For all *in vitro* studies, resistant cells were maintained in gefitinib- or erlotinib-free medium for at least 2 weeks before experiments, to eliminate the effects of the drugs. Gefitinib-resistant cells are referred to as HCC827/GR.

Kinase inhibition profile

The *in vitro* NPS-1034 profile of inhibition of RTKs was analyzed using DiscoveRx and Carna Bioscience RTK assay kits according to the manufacturer's protocols (see also the protocol described in Supplementary Materials and Methods).

Cell viability assays

To perform the MTT assay, cells (0.5×10^4/well) were plated in 96-well sterile plastic plates and allowed to attach overnight. Cells were exposed to varying doses of gefitinib, erlotinib, PHA-665752, and NPS-1034 in medium containing 1% FBS. After 72 hours, 15 μL of MTT solution (5 mg/mL) was added to each well and plates were incubated for 4 hours. Crystalline formazan was solubilized with 100 μL of a 10% (w/v) SDS solution for 24 hours. Absorbance at 595 nm was read spectrophotometrically using a microplate reader.

To validate the long-term effects of a combination of EGFR-TKIs and NPS-1034, cells were treated with the indicated doses of drugs for 72 hours, and the medium was replaced with drug-free medium. After incubation for 5 days, attached cells were stained with a 0.2% trypan blue solution containing 50% methanol. The plate was washed under running tap water and allowed to dry. The viability (living and dead cells) of cells was determined using an ADAM-MC automatic cell counter (NanoEnTek), according to the manufacturer's instructions.

The combination effect was evaluated by MTT assay at a 1:1 ratio of each drug. CI values were processed using the CalcuSyn software (Biosoft). CI values <1, = 1, and >1 indicated synergism, additive effect, and antagonism, respectively.

Western blotting

Cells were lysed in buffer containing 137 mmol/L NaCl, 15 mmol/L EGTA, 0.1 mmol/L sodium orthovanadate, 15 mmol/L $MgCl_2$, 0.1% Triton X-100, 25 mmol/L MOPS, 100 μmol/L phenylmethylsulfonyl fluoride, and 20 μmol/L leupeptin, adjusted to pH 7.2. Proteins were separated on SDS-polyacrylamide gels and electrotransferred to Immobilon-P membranes (Millipore). Antibodies specific for p-EGFR (Tyr1173), EGFR, MET, p-Akt (Ser 473), Akt, ERK, P-Tyr (PY99), and actin were obtained from Santa Cruz Biotechnology; those for p-MET (Tyr1234/1235), p-ERK (Thr202/Tyr204), caspase-3, and PARP-1 were purchased from Cell Signaling Technology; and those for p-AXL and AXL were purchased from R&D system. To evaluate the level of phosphorylated AXL, lysates were immunoprecipitated with an anti-AXL antibody and immunoblotted with an anti-phosphotyrosine (p-Tyr) antibody. Proteins were detected with an enhanced chemiluminescence Western blotting kit (Amersham Biosciences), according to the manufacturer's instructions.

Small interfering RNA transfection

Silencer-validated small interfering RNAs (siRNA) for EGFR, AXL, MET, and control were purchased from Santa Cruz Biotechnology. H820 cells were seeded into 60 mm dishes and allowed to attach overnight. A 10 μL (100 nmol/L) aliquot of siRNA solution (10 μmol/L) and 5 μL of the Lipofectamine RNAiMAX Reagent (Invitrogen) were each mixed with 100 μL of serum-free RPMI 1640 medium. Solutions were incubated for 20 minutes at room temperature after combining the 2 mixtures and added to the cells. After transfection, the suppression of targeted proteins was determined by Western blotting. The viability of cells was determined by trypan blue staining using an ADAM-MC automatic cell counter.

In vivo study

Female severe combined immunodeficiency (SCID) mice (17–20 g, 6 weeks of age) were purchased from Charles River Laboratories. Tumors were grown by implanting 5×10^6 cells in Matrigel (BD Biosciences) into the mouse flanks. Treatment of 5 mice per group was started when the tumors had reached a volume of 50 to 100 mm^3 with vehicle control, gefitinib (100 mg/kg, 5 days a week), NPS-1034 (10 mg/kg, 5 days a week),

Published OnlineFirst October 28, 2013; DOI: 10.1158/0008-5472.CAN-13-1103

PHA-665752 (12.5 mg/kg, 5 days a week), gefitinib plus PHA-665752, or gefitinib plus NPS-1034. Gefitinib and NPS-1034 were administered orally, and PHA-665752 was given intravenously via tail vein injections. Treatment was stopped at the indicated day and mice were followed-up for tumor recurrence. To measure tumor size, the length (L) and width (W) of the tumor were measured with calipers, and tumor volume (TV) was calculated as $TV = (L \times W^2)/2$. Immunohistochemical staining was performed using a specific primary antibody (Ki-67; Dako-Cytomation), the EnVision Plus staining kit (DakoCytomation), and the APO-Direct terminal deoxynucleotidyl transferase–mediated dUTP nick end labeling (TUNEL) assay kit (Millipore), according to the suppliers' instructions. Quantitative analysis of section staining was performed by counting immunopositive cells in 5 arbitrarily selected fields at ×40 magnification.

Results

Development of NPS-1034 and its kinase inhibition profile

We initially designed and synthesized NPS-1034 (Fig. 1) as a MET inhibitor. However, we found that NPS-1034 also inhibited several other kinases, as assessed by the ATP competition assay. As shown in Table 1, NPS-1034 showed significant inhibitory activity against AXL, CSF1R, DDR, FLT3, KIT, MERTK, MET, MST1R, ROS, TIE1, and TRK in an assay that used 1 μmol/L ATP. In particular, NPS-1034 inhibited AXL (IC_{50}, 10.3 nmol/L) and MET (IC_{50}, 48 nmol/L, data not shown). Using cellular phosphorylation assays, we confirmed that NPS-1034 inhibited other kinases, such as FLT3, KIT, and DDR1 (Supplementary Fig. S1). Although NPS-1034 has inhibitory activity on various kinases, it may be most useful as a dual inhibitor of AXL and MET.

Combined treatment with NPS-1034 and gefitinib overcomes the drug resistance caused by *MET* gene amplification

A gefitinib-resistant subline that was derived from the parental drug-sensitive HCC827 cell line was established by continuous exposure of cells to gefitinib more than a period of 8 months. The resistant subline was designated HCC827/GR and exhibited a 1,000-fold higher resistance to gefitinib than the parental cells (gefitinib IC_{50}, <0.01 μmol/L in HCC827 cells and >10 μmol/L in HCC827/GR cells; Fig. 2A). Consistent with a prior study, we also observed increased total MET protein and gene amplification in HCC827/GR cells (Fig. 2B and data not shown). The combination of gefitinib and a MET inhibitor, PHA 665752, effectively inhibited the growth of HCC827/GR cells, whereas neither of the agents alone led to growth inhibition (Fig. 2C, top). In addition, the combination of gefitinib and NPS-1034 also effectively inhibited the growth of HCC827/GR cells (Fig. 2C, bottom). A similar synergistic

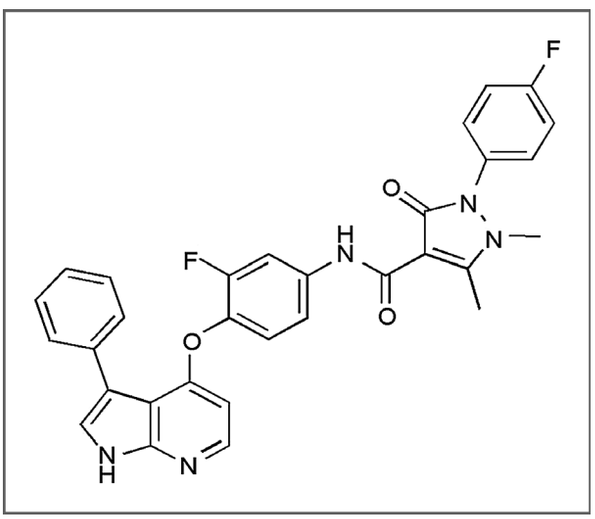

Figure 1. Chemical structure of NPS-1034.

Table 1. NPS-1034 as a multikinase inhibitor

FLT1	ABL1(E255K)-phosphorylated
FLT3	ABL1(F317I)-nonphosphorylated
FLT3(D835H)	ABL1(F317I)-phosphorylated
FLT3(D835Y)	ABL1(F317L)-nonphosphorylated
FLT3(ITD)	ABL1(F317L)-phosphorylated
FLT3(K663Q)	ABL1(H396P)-nonphosphorylated
FLT3(N841I)	ABL1(H396P)-phosphorylated
FLT3(R834Q)	ABL1(M351T)-phosphorylated
FLT4	ABL1(Q252H)-nonphosphorylated
FRK	ABL1(Q252H)-phosphorylated
FYN	ABL1(T315I)-nonphosphorylated
HCK	ABL1(T315I)-phosphorylated
IGF1R	ABL1(Y253F)-phosphorylated
INSR	ABL1-nonphosphorylated
INSRR	ABL1-phosphorylated
ITK	ABL2
JAK1(JH1domain-catalytic)	ALK
JAK1(JH2domain-pseudokinase)	AXL
JAK2(JH1domain-catalytic)	BLK
JAK3(JH1domain-catalytic)	BMX
KIT	BRK
KIT(A829P)	BTK
KIT(D816H)	CSF1R
KIT(D816V)	CSK
KIT(L576P)	CTK
KIT(V559D)	DDR1
KIT(V559D,T670I)	DDR2
KIT(V559D,V654A)	EGFR
LCK	EGFR(E746-A750del)
LTK	EGFR(G719C)
LYN	EGFR(G719S)
MERTK	EGFR(L747-E749del, A750P)
MET	EGFR(L747-S752del, P753S)
MET(M1250T)	EGFR(L747-T751del,Sins)
MET(Y1235D)	EGFR(L858R)
MST1R	EGFR(L858R,T790M)
MUSK	EGFR(L861Q)
PDGFRA	EGFR(S752-I759del)
PDGFRB	EGFR(T790M)
PYK2	EPHA1
RET	EPHA2
RET(M918T)	EPHA3
RET(V804L)	EPHA4
RET(V804M)	EPHA5
ROS1	EPHA6
SRC	EPHA7
SRMS	EPHA8
SYK	EPHB1
TEC	EPHB2
TIE1	EPHB3
TIE2	EPHB4
TNK1	EPHB6
TNK2	ERBB2
TRKA	ERBB3
TRKB	ERBB4
TRKC	FAK
TXK	FER
TYK2(JH1domain-catalytic)	FES
TYK2(JH2domain-pseudokinase)	FGFR1
TYRO3	FGFR2
VEGFR2	FGFR3
YES	FGFR3(G697C)
ZAP70	FGFR4
	FGR

Red: 90~99% inhibition Yellow: 70~90% inhibition
Light green: 50~70% inhibition Green: <50% inhibition

Published OnlineFirst October 28, 2013; DOI: 10.1158/0008-5472.CAN-13-1103

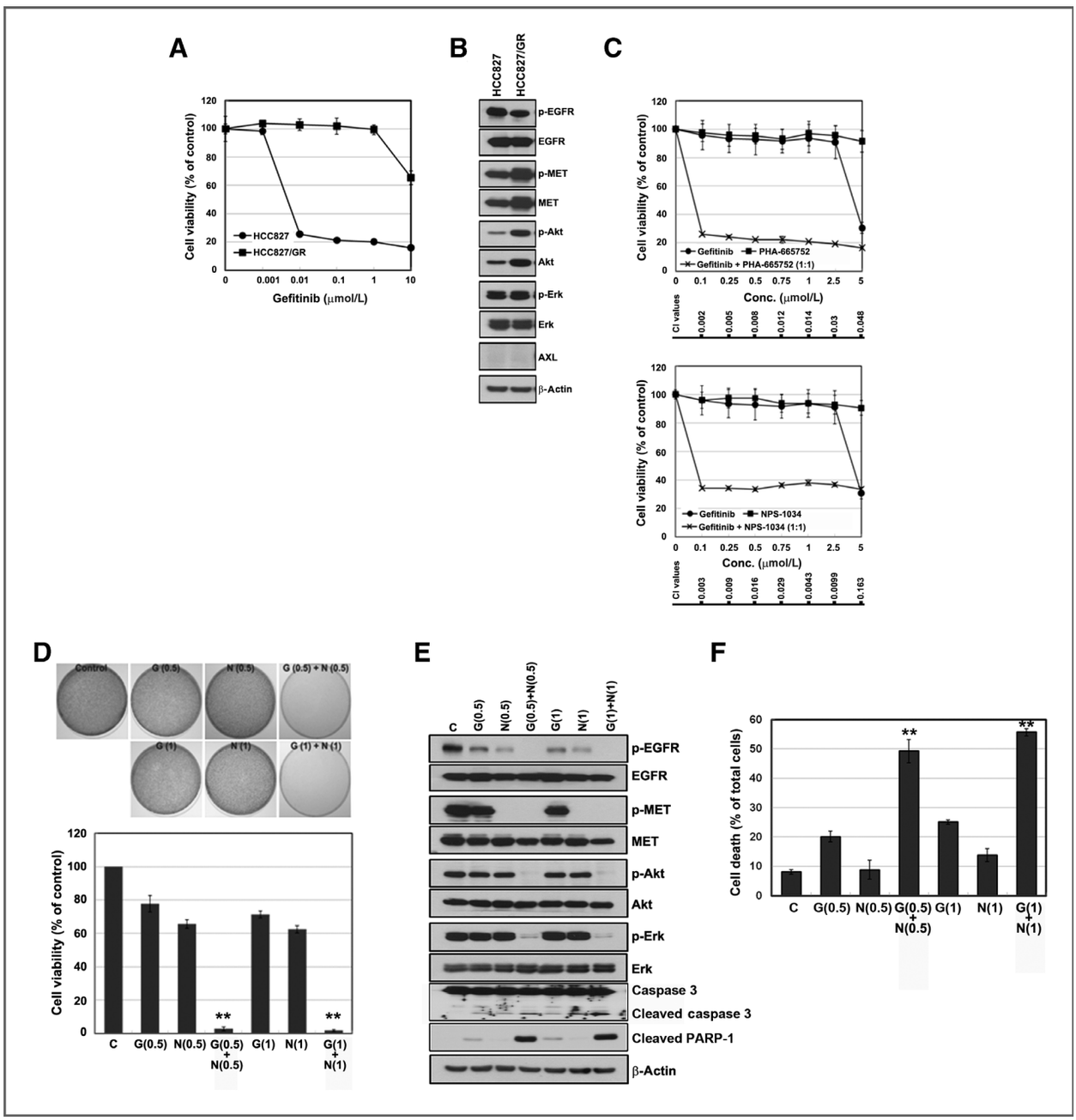

Figure 2. Effects of combined treatment with gefitinib and NPS-1034 in HCC827/GR cells with MET gene amplification. A, the viability of cells was determined using the MTT assay. B, the basal expression of EGFR, MET, and their downstream molecules was determined by Western blotting. C, HCC827/GR cells were treated with gefitinib, PHA-665752, NPS-1034, or a combination of gefitinib with one of the other 2 drugs for 72 hours. Combined effects were measured using the MTT assay and CI values. D, HCC827/GR cells were treated with the indicated doses (μmol/L) of drugs for 72 hours, and the medium was replaced with drug-free medium. After incubation for 5 days, attached cells were stained with trypan blue solution (top). The bottom graph shows cell viability based on cell counting. The results are representative of at least 3 independent experiments, and the error bars signify standard deviations (± SDs). E and F, HCC827/GR cells were treated with drugs, as in D. After 48 hours, cells were harvested and subjected to Western blotting using the antibodies described in E. After 72 hours, cell death was assessed as described in Materials and Methods (F). Results are representative of at least three independent experiments, and the error bars signify standard deviations (± SDs). **, $P < 0.001$ for the combination of gefitinib plus NPS-1034 versus either control or drug alone. C, control; G, gefitinib; N, NPS-1034.

effect was observed across the full range of doses tested. Although a single treatment with NPS-1034 did not show significant antiproliferative effects in the long-term exposure experiment, combined NPS-1034 and gefitinib treatment overcame gefitinib resistance via the inhibition of the phosphorylation of MET, Akt, and Erk, as well as modest EGFR

Published OnlineFirst October 28, 2013; DOI: 10.1158/0008-5472.CAN-13-1103

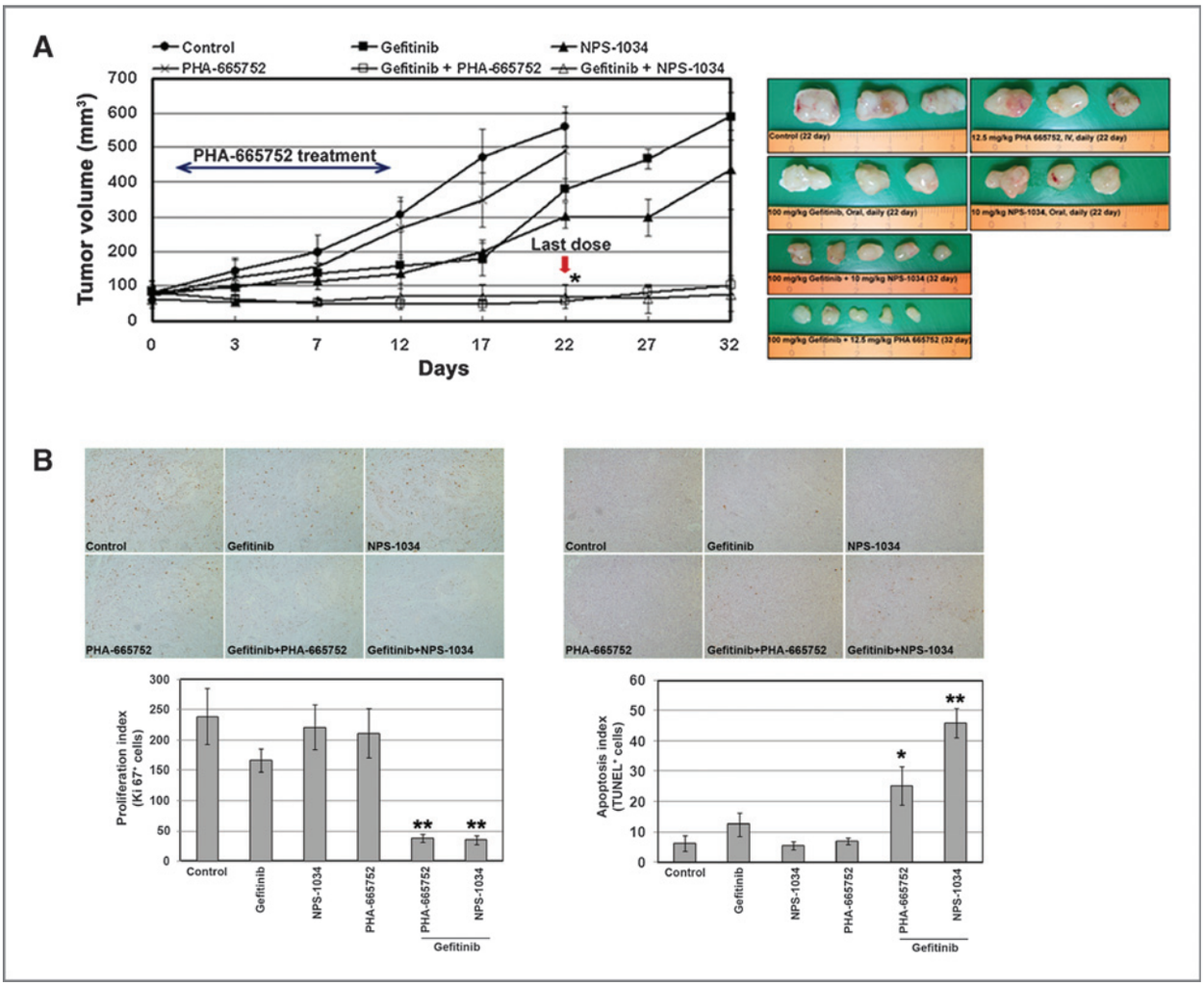

Figure 3. Addition of NPS-1034 to gefitinib overcomes acquired resistance to gefitinib in a xenograft model. A, SCID mice bearing established HCC827/GR tumor cell xenografts were treated with each drug, as described in Materials and Methods. The length and width of the tumors were measured at the days indicated and tumor volumes were calculated. The bars represent mean tumor volume ± SD. B, immunohistochemical staining for Ki-67 and TUNEL, as described in Materials and Methods. Quantitative data for proliferation and apoptotic indices are shown as Ki-67$^+$ cells (left) and TUNEL$^+$ cells (right). *, $P < 0.01$ and **, $P < 0.001$ for the combination of gefitinib plus NPS-1034 or gefitinib plus PHA-665752 versus either the control or drug alone.

phosphorylation, which was maintained in the presence of gefitinib alone (Fig. 2D and E). Furthermore, treatment with a combination of gefitinib and NPS-1034 induced caspase-3 and PARP-1 cleavage, thus leading to enhanced cell death (Fig. 2F).

To evaluate further, the antitumor efficacy of the combination of NPS-1034 or PHA-665752 with gefitinib, an HCC827/GR tumor xenograft was established in SCID mice. PHA-665752 treatment was limited to 12 days to avoid the venous toxicity associated with a longer administration of the drug (24). Although a single treatment produced a slight decrease in tumor growth, combined treatment resulted in substantial growth inhibition (Fig. 3A). The efficacy of tumor inhibition was not significantly different between gefitinib plus PHA-665752 and gefitinib plus NPS-1034. Moreover, the inhibition of tumor growth persisted in the combination groups for 10 days after the discontinuation of the drugs. Consistent with the observations about tumor size, the combination resume (gefitinib plus PHA-665752 and gefitinib plus NPS-1034) led to the inhibition of tumor proliferation and the induction of apoptosis (Fig. 3B). Interestingly, gefitinib plus NPS-1034 induced increased apoptosis to a greater extent than did gefitinib plus PHA-665752.

Addition of NPS-1034 to erlotinib overcomes AXL-mediated drug resistance

We reported recently that increased activation of AXL led to EGFR-TKI resistance in HCC827/ER cells (23). This erlotinib-resistant subline exhibited IC_{50} values for erlotinib that were more than 1,000-fold larger than those of the parental HCC827 cells (Fig. 4A). The expression and activity of AXL was significantly increased in HCC827/ER cells, and NPS-1034 treatment effectively inhibited its tyrosine phosphorylation (Fig. 4B and C). When HCC827/ER cells were treated with erlotinib and PHA-665752 or erlotinib and NPS-1034; NPS-1034 restored

Published OnlineFirst October 28, 2013; DOI: 10.1158/0008-5472.CAN-13-1103

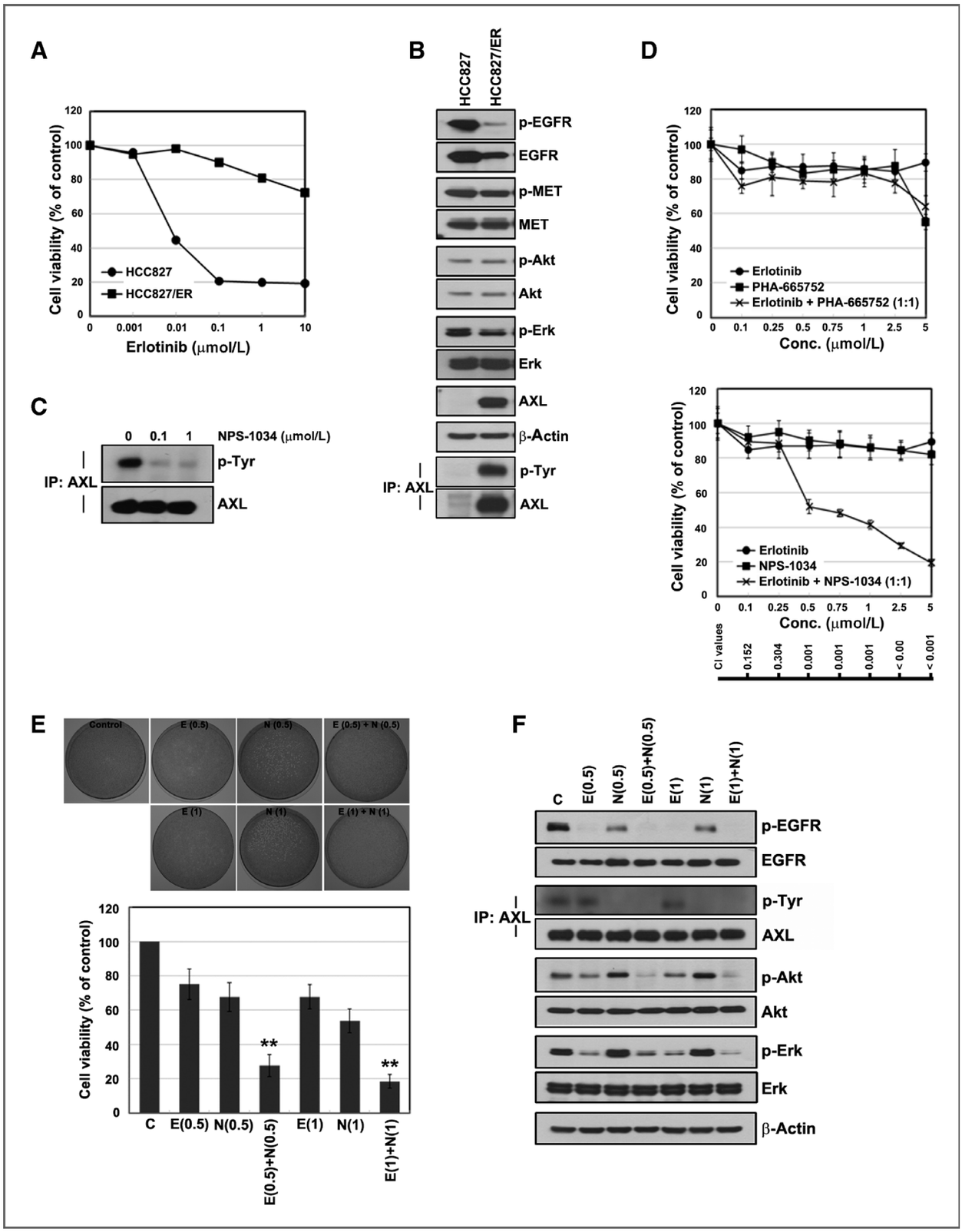

Figure 4. Effects of combined treatment with erlotinib and NPS-1034 in HCC827/ER cells with AXL activation. A, the viability of cells was determined using the MTT assay. B, the basal levels of EGFR, MET, AXL, and their downstream molecules were determined by Western blotting. C, HCC827/ER cells were treated with the indicated doses of NPS-1034 for 3 hours. Lysates were immunoprecipitated with an anti-AXL antibody and immunoblotted with antibodies for phosphotyrosine (p-Tyr) and AXL. D–F, HCC827/ER cells were treated with erlotinib and experiments were performed as in Fig. 2D–F. C, control; E, erlotinib; N, NPS-1034. **, $P < 0.001$ for the combination of erlotinib plus NPS-1034 versus either the control or drug alone.

Published OnlineFirst October 28, 2013; DOI: 10.1158/0008-5472.CAN-13-1103

sensitivity to erlotinib, whereas PHA-665752 did not (Fig. 4D). Consistent with what was observed for HCC827/GR cells, combined NPS-1034 and erlotinib treatment overcame erlotinib resistance via the complete inhibition of signaling downstream from EGFR (Fig. 4E and F). Although the induction of cell death by the combination treatment was not significantly increased in this dose frame, a higher dose of NPS-1034 (2.5 μmol/L) led to enhanced cell death (Supplementary Fig. S2).

NPS-1034 treatment enhances sensitivity to EGFR-TKIs in H820 cells

A previous study showed that XL880 affected the viability of H820 cells harboring a sensitizing deletion (del E746-E749) mutation, the resistant T790M mutation, and *MET* amplification (12). The role of MET in the resistance of H820 cells to EGFR-TKIs was emphasized, as an irreversible EGFR inhibitor, CL-387,785 (which has the capability to overcome T790M-mediated resistance), did not suppress the proliferation of H820 cells. In agreement with a previous study (12), we also observed that the H820 cell line was resistant to reversible EGFR-TKIs (gefitinib and erlotinib) and to an irreversible EGFR-TKI (afatinib; Supplementary Fig. S3). However, because XL880 inhibited AXL as well as MET, we investigated whether the overcoming effect of XL880 in this cell line was mediated by suppression of MET. Unexpectedly, treatment with PHA-665752, a relatively specific MET inhibitor, failed to overcome the resistance to gefitinib or erlotinib, whereas a combination treatment with NPS-1034 exerted significant effects (Fig. 5A and B). This differential effect led us to evaluate both MET and AXL in H820 cells. The levels of expression and activation of MET in H820 cells were consistent with data published previously (12). Interestingly, AXL was highly expressed and activated in H820 cells, similar to what was observed in HCC827/ER cells (Fig. 5C and D).

To identify the major factor involved in resistance to gefitinib or erlotinib, we transfected H820 cells with EGFR, MET, or AXL siRNAs, followed by gefitinib or erlotinib treatment. As shown in Fig. 5E and F, each siRNA effectively suppressed the targeted gene, but did not result in significant inhibition of cell growth. However, we found that AXL siRNA-transfected H820 cells became the most sensitive to the effects of gefitinib or erlotinib. NPS-1034 treatment inhibited MET as well as AXL activity in H820 cells, and a combined treatment with EGFR-TKIs completely suppressed EGFR downstream signaling and led to enhanced cell death (Fig. 5G and H). These results indicate that AXL makes the major contribution to the resistance to EGFR-TKIs observed in H820 cells.

NPS-1034 inhibits ROS1 activity and cell proliferation in HCC78 cells

We observed that NPS-1034 inhibited ROS1 activity (Table 1). Therefore, we examined whether NPS-1034 can inhibit ROS1 activity and cell proliferation in HCC78 cells with a ROS1 rearrangement. As shown in Fig. 6A, NPS-1034 treatment inhibited cell proliferation so that the degree of growth inhibition was similar to that produced by crizotinib. Although the efficacy of growth inhibition was not different for the 2 drugs, NPS-1034 exhibited more potent inhibition of ROS1 activity than crizotinib (Fig. 6B). These results indicate that NPS-1034 is a candidate for clinical application to the treatment of NSCLC with ROS1 rearrangement.

Discussion

We observed that the resistance mechanisms to several EGFR-TKIs share common pathways, such as the induction of steric hindrance of drug binding by secondary mutations and the activation of redundant pathways to maintain downstream signals in case of blocking main addicted signaling pathway, although the specific mutations and bypass signals may differ. Our study demonstrated that NPS-1034 is effective in NSCLC cells with resistance to EGFR-TKIs via the bypass signals of MET or AXL.

AXL was identified as a "tyrosine kinase switch" that causes imatinib resistance in gastrointestinal stromal tumors (GIST). Imatinib-resistant GIST cells alter their survival signal from c-KIT to AXL and overexpress its ligand, Gas6 (22). In addition to preclinical evidence, downregulation of c-KIT and activation of AXL were confirmed in GIST patients displaying resistance to imatinib. Furthermore, overexpression of AXL conferred drug resistance in acute myeloid leukemia, and was induced after exposure to chemotherapeutic drugs (20). Liu and colleagues reported that AXL overexpression constitutes a novel mechanism of lapatinib resistance in HER2-positive breast cancer cells. An siRNA against AXL restored the sensitivity to lapatinib in these resistant cells (21). Thus, AXL seems to be an important redundant RTK that induces resistance to many targeted agents, especially when we also consider that our previous study demonstrated its role in EGFR-mutant NSCLC cells with acquired resistance to EGFR-TKIs.

H820 cells harbor the sensitizing *EGFR* deletion mutation in exon 19, the T790M mutation, as well as *MET* amplification (12). H820 cells are not responsive to EGFR-TKIs, although these cells were isolated from a patient who had never been exposed to that type of drug. Because irreversible EGFR-TKIs were reported to be active against T790M, and H820 cells exhibit resistance to both erlotinib and an irreversible EGFR inhibitor (CL-387, 785), a previous report suggested that T790M does not contribute to resistance in H820 cells (12). This is possible, as we have observed that a low level of T790M is not sufficient to cause resistance, and that the T790M allele is present at a frequency of only 7% in H820 cells, as assessed using a scorpion-amplification refractory mutation system, compared with 55% in H1975 cells, in which T790M is the main resistance mechanism (10). Furthermore, we showed that specific inhibition of EGFR by siRNA had only a marginal growth-inhibitory effect on H820 cells, indicating that these cells may escape from EGFR dependency and use signals other than EGFR.

However, H820 cells are sensitive to XL880, which has a potent activity against MET (10). Based on studies of the characteristics of H820 cells, Bean and colleagues concluded that MET alteration is the main resistance mechanism, that it occurs independently of T790M mutations, and that MET may be a relevant therapeutic target in these cells. Although some of these theories are valid, data from our experiments showed

Published OnlineFirst October 28, 2013; DOI: 10.1158/0008-5472.CAN-13-1103

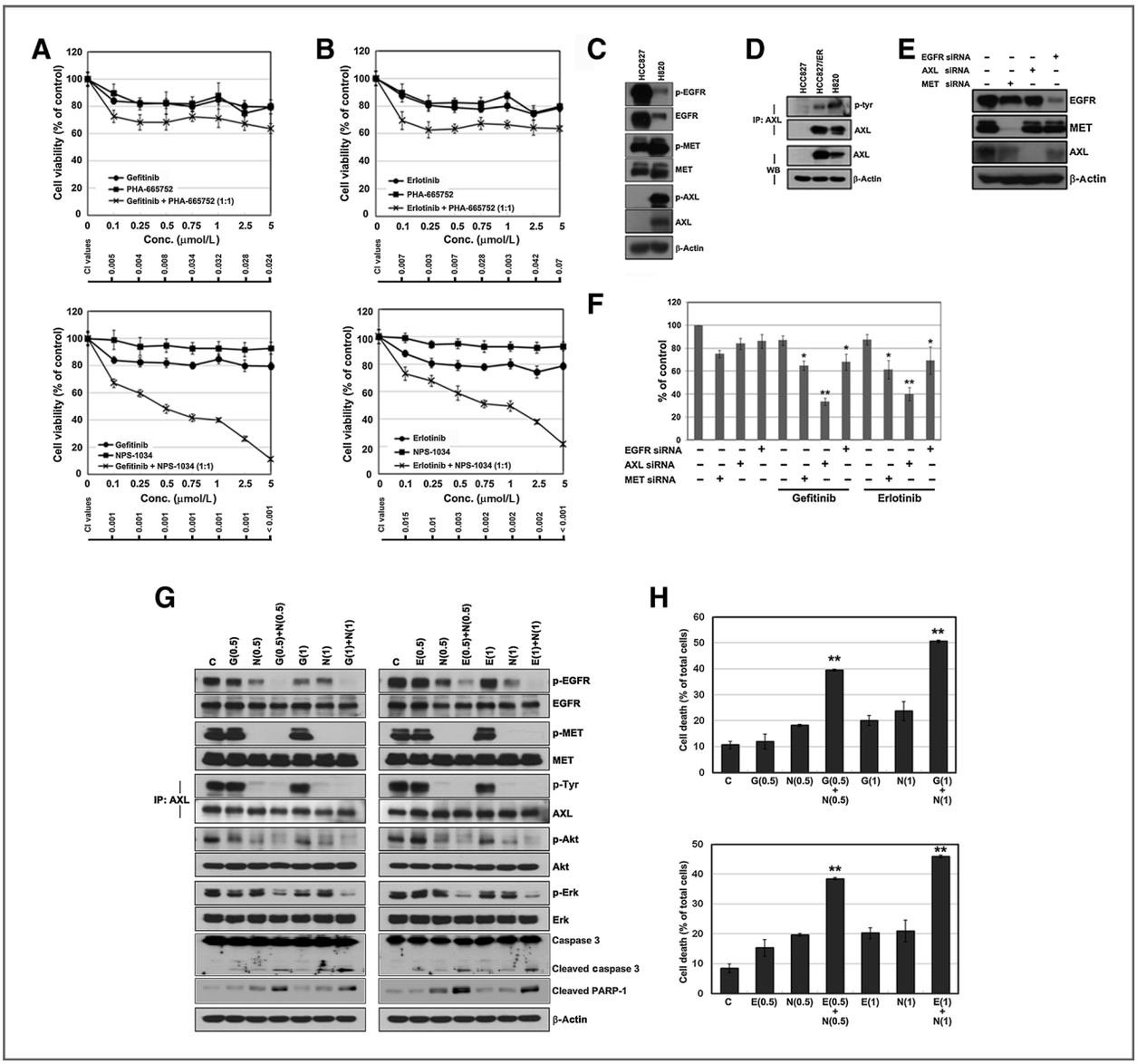

Figure 5. Correlation between AXL activation and resistance to EGFR-TKIs in H820 cells. A and B, H820 cells were treated with gefitinib, erlotinib, PHA-665752, NPS-1034, or a combination of the 2 drugs. Combined effects were measured using the MTT assay. C and D, the basal levels of proteins and endogenous activities of AXL were determined by Western blotting. E and F, H820 cells were transfected with the indicated siRNA and gene knockdown was confirmed by Western blotting (E). After transfection, cells were treated with the indicated drugs (100 nmol/L) for 48 hours and then counted (F). Results are representative of at least 3 independent experiments, and the error bars signify standard deviations (± SDs). *, $P < 0.01$ and **, $P < 0.001$ for the combination of gefitinib or erlotinib plus indicated siRNA versus either the control, indicated siRNA, or drug alone. G and H, H820 cells were treated with the indicated drugs. After 48 hours, cells were harvested and subjected to Western blotting using the antibodies described in the figure (G). After 72 hours, cell death was assessed as described in Materials and Methods (H). Results are representative of at least three independent experiments, and the error bars signify standard deviations (± SDs). **, $P < 0.001$ for the combination of gefitinib or erlotinib plus NPS-1034 versus either the control or drug alone. C, control; G, gefitinib; N, NPS-1034.

that H820 cell proliferation was not inhibited by a combination of erlotinib and another MET inhibitor (PHA665752), raising doubts about whether MET constitutes the main resistance mechanism in these cells. We established another gefitinib-resistant HCC827 cell line (HCC827/GR) with characteristics similar to those generated by Engelman and colleagues (11). This cell line displayed *MET* amplification without AXL activation, and its growth was inhibited by a combination treatment with gefitinib and PHA665752. This finding indicates that PHA665752 is sufficient to overcome the resistance induced by the MET bypass signal. Therefore, the different effects of XL880 and PHA665752 on H820 cell proliferation do not seem to be caused by their ability to inhibit MET. Rather, other targets of XL880, such as AXL and VEGFR, may be the real cause of resistance, considering that XL880 is a multikinase inhibitor. We revealed for the first time that AXL expression is also

Published OnlineFirst October 28, 2013; DOI: 10.1158/0008-5472.CAN-13-1103

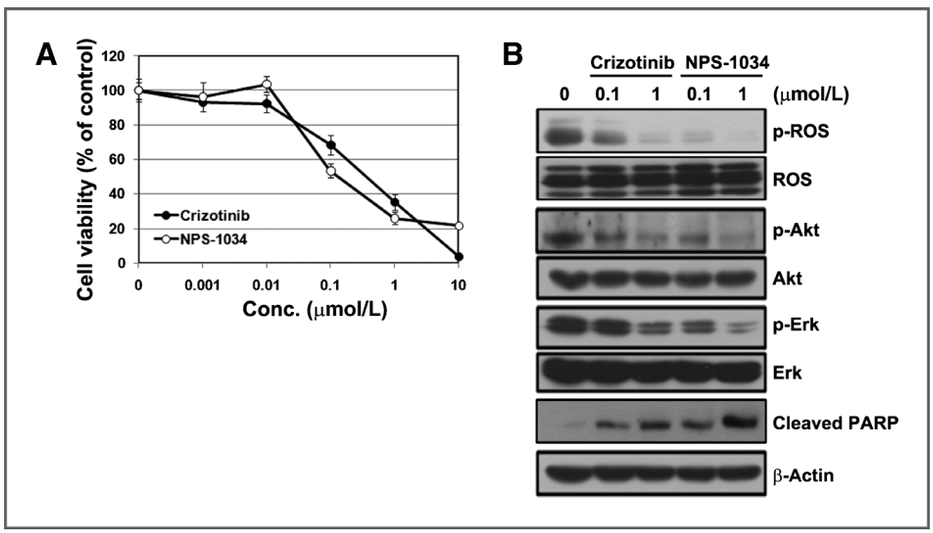

Figure 6. NPS-1034 treatment inhibited ROS1 activity. A, HCC-78 cells treated with the indicated doses of crizotinib or NPS-1034 for 72 hours. The viability of cells was determined using the MTT assay. B, cells treated with or without the indicated doses of crizotinib or NPS-1034 for 24 hours. Changes in ROS, Akt, and Erk activity and cleaved PARP were analyzed by Western blotting.

increased in H820 cells, and that cell proliferation is suppressed by NPS-1034, but not by a specific MET inhibitor, which provides additional evidence in support of a possible role for AXL in resistance to EGFR-TKIs.

Interestingly, the majority of signals examined, including EGFR, Her2, and Her3, were downregulated in HCC827/ER cells (data not shown). Nevertheless, the EGFR signal seems to be important, as the single inhibition of AXL via XL880 or siRNA transfection failed to suppress cell proliferation sufficiently in erlotinib-resistant cells. Both inhibition of EGFR and AXL effectively modulated cell viability and Akt phosphorylation, indicating that the signaling pathway involved in cell survival is not completely switched from EGFR to AXL, and that both signals may contribute to the survival and proliferation of erlotinib-resistant cells. Disappointingly, we failed to establish a subcutaneous xenograft mouse model using HCC827/ER cells. It is not certain whether the downregulation of many signals led to engraftment failure of these cells in the mouse.

As shown in Table 1, NPS-1034 is a multikinase inhibitor. Among its targets, ROS1 was identified recently as an oncogenic driver of NSCLC in the case of fusion with TPM3, SDC4, SLC34A2, EZR, and CD74 (25, 26). Lung cancer with ROS1 rearrangement represents a unique, clinically important subset, although its prevalence seems to be less than 5% of NSCLC. Bergethon and colleagues reported a dramatic response in a patient with ROS1 rearrangement to treatment with crizotinib, which is a multikinase inhibitor that targets MET, AXL, and ROS1 and is currently being used to treat NSCLC with ALK rearrangement (27, 28). We found that NPS-1034 is more active than crizotinib in inhibiting ROS1 activity, suggesting its possible clinical application to the treatment of NSCLC with ROS1 rearrangement.

In conclusion, NPS-1034 is a very active agent in EGFR-mutant NSCLC with resistance to EGFR-TKIs via the bypass signals of MET or AXL and in ROS1-rearranged NSCLC.

Disclosure of Potential Conflicts of Interest

No potential conflicts of interest were disclosed.

Authors' Contributions

Conception and design: J.K. Rho, Y.J. Choi, T.W. Kim, E.K. Choi, S.-J. Yoon, B.M. Park, C.-M. Choi, J.C. Lee

Acquisition of data (provided animals, acquired and managed patients, provided facilities, etc.): J.K. Rho, Y.J. Choi, S.Y. Kim, S.-J. Yoon, J.H. Bae, C.-M. Choi

Analysis and interpretation of data (e.g., statistical analysis, biostatistics, computational analysis): J.K. Rho, Y.J. Choi, S.Y. Kim, S.-J. Yoon, J.C. Lee

Writing, review, and/or revision of the manuscript: J.K. Rho, Y.J. Choi, S.-J. Yoon, C.-M. Choi, J.C. Lee

Administrative, technical, or material support (i.e., reporting or organizing data, constructing databases): Y.J. Choi, T.W. Kim, S.-J. Yoon, B.M. Park, J.H. Bae

Study supervision: E.K. Choi, C.-M. Choi, J.C. Lee

Grant Support

This study was supported by a grant of the Korean Health Technology R&D Project, Ministry of Health & Welfare (A102059), and a grant of the Korea Drug Development Fund (KDDF-201111-02), Republic of Korea.

The costs of publication of this article were defrayed in part by the payment of page charges. This article must therefore be hereby marked *advertisement* in accordance with 18 U.S.C. Section 1734 solely to indicate this fact.

Received April 19, 2013; revised August 16, 2013; accepted September 2, 2013; published OnlineFirst October 28, 2013.

References

1. Kris MG, Natale RB, Herbst RS, Lynch TJ Jr., Prager D, Belani CP, et al. Efficacy of gefitinib, an inhibitor of the epidermal growth factor receptor tyrosine kinase, in symptomatic patients with non-small cell lung cancer: a randomized trial. JAMA 2003;290:2149–58.
2. Perez-Soler R. Phase II clinical trial data with the epidermal growth factor receptor tyrosine kinase inhibitor erlotinib (OSI-774) in non-small-cell lung cancer. Clin Lung Cancer 2004;6 Suppl 1:S20–3.
3. Lynch TJ, Bell DW, Sordella R, Gurubhagavatula S, Okimoto RA, Brannigan BW, et al. Activating mutations in the epidermal growth

Published OnlineFirst October 28, 2013; DOI: 10.1158/0008-5472.CAN-13-1103

factor receptor underlying responsiveness of non-small-cell lung cancer to gefitinib. N Engl J Med 2004;350:2129–39.
4. Paez JG, Janne PA, Lee JC, Tracy S, Greulich H, Gabriel S, et al. EGFR mutations in lung cancer: correlation with clinical response to gefitinib therapy. Science 2004;304:1497–500.
5. Sharma SV, Bell DW, Settleman J, Haber DA. Epidermal growth factor receptor mutations in lung cancer. Nat Rev Cancer 2007;7:169–81.
6. Sharma SV, Gajowniczek P, Way IP, Lee DY, Jiang J, Yuza Y, et al. A common signaling cascade may underlie "addiction" to the Src, BCR-ABL, and EGF receptor oncogenes. Cancer Cell 2006;10:425–35.
7. Sordella R, Bell DW, Haber DA, Settleman J. Gefitinib-sensitizing EGFR mutations in lung cancer activate anti-apoptotic pathways. Science 2004;305:1163–7.
8. Kobayashi S, Boggon TJ, Dayaram T, Janne PA, Kocher O, Meyerson M, et al. EGFR mutation and resistance of non-small-cell lung cancer to gefitinib. N Engl J Med 2005;352:786–92.
9. Perez-Soler R, Chachoua A, Hammond LA, Rowinsky EK, Huberman M, Karp D, et al. Determinants of tumor response and survival with erlotinib in patients with non–small-cell lung cancer. J Clin Oncol 2004;22:3238–47.
10. Yun CH, Mengwasser KE, Toms AV, Woo MS, Greulich H, Wong KK, et al. The T790M mutation in EGFR kinase causes drug resistance by increasing the affinity for ATP. Proc Natl Acad Sci U S A 2008;105:2070–5.
11. Engelman JA, Zejnullahu K, Mitsudomi T, Song Y, Hyland C, Park JO, et al. MET amplification leads to gefitinib resistance in lung cancer by activating ERBB3 signaling. Science 2007;316:1039–43.
12. Bean J, Brennan C, Shih JY, Riely G, Viale A, Wang L, et al. MET amplification occurs with or without T790M mutations in EGFR mutant lung tumors with acquired resistance to gefitinib or erlotinib. Proc Natl Acad Sci U S A 2007;104:20932–7.
13. Pao W, Miller VA, Politi KA, Riely GJ, Somwar R, Zakowski MF, et al. Acquired resistance of lung adenocarcinomas to gefitinib or erlotinib is associated with a second mutation in the EGFR kinase domain. PLoS Med 2005;2:e73.
14. Linger RM, Keating AK, Earp HS, Graham DK. TAM receptor tyrosine kinases: biologic functions, signaling, and potential therapeutic targeting in human cancer. Adv Cancer Res 2008;100:35–83.
15. Hafizi S, Dahlback B. Signalling and functional diversity within the Axl subfamily of receptor tyrosine kinases. Cytokine Growth Factor Rev 2006;17:295–304.
16. Ishimoto Y, Ohashi K, Mizuno K, Nakano T. Promotion of the uptake of PS liposomes and apoptotic cells by a product of growth arrest-specific gene, gas6. J Biochem 2000;127:411–7.
17. Li Y, Ye X, Tan C, Hongo JA, Zha J, Liu J, et al. Axl as a potential therapeutic target in cancer: role of Axl in tumor growth, metastasis and angiogenesis. Oncogene 2009;28:3442–55.
18. Lemke G, Rothlin CV. Immunobiology of the TAM receptors. Nat Rev Immunol 2008;8:327–36.
19. Shankar SL, O'Guin K, Kim M, Varnum B, Lemke G, Brosnan CF, et al. Gas6/Axl signaling activates the phosphatidylinositol 3-kinase/Akt1 survival pathway to protect oligodendrocytes from tumor necrosis factor alpha-induced apoptosis. J Neurosci 2006;26:5638–48.
20. Hong CC, Lay JD, Huang JS, Cheng AL, Tang JL, Lin MT, et al. Receptor tyrosine kinase AXL is induced by chemotherapy drugs and overexpression of AXL confers drug resistance in acute myeloid leukemia. Cancer Lett 2008;268:314–24.
21. Liu L, Greger J, Shi H, Liu Y, Greshock J, Annan R, et al. Novel mechanism of lapatinib resistance in HER2-positive breast tumor cells: activation of AXL. Cancer Res 2009;69:6871–8.
22. Mahadevan D, Cooke L, Riley C, Swart R, Simons B, Della Croce K, et al. A novel tyrosine kinase switch is a mechanism of imatinib resistance in gastrointestinal stromal tumors. Oncogene 2007;26:3909–19.
23. Zhang Z, Lee JC, Lin L, Olivas V, Au V, LaFramboise T, et al. Activation of the AXL kinase causes resistance to EGFR-targeted therapy in lung cancer. Nat Genet 2012;44:852–60.
24. Christensen JG, Schreck R, Burrows J, Kuruganti P, Chan E, Le P, et al. A selective small molecule inhibitor of c-Met kinase inhibits c-Met-dependent phenotypes *in vitro* and exhibits cytoreductive antitumor activity *in vivo*. Cancer Res 2003;63:7345–55.
25. Rikova K, Guo A, Zeng Q, Possemato A, Yu J, Haack H, et al. Global survey of phosphotyrosine signaling identifies oncogenic kinases in lung cancer. Cell 2007;131:1190–203.
26. Takeuchi K, Soda M, Togashi Y, Suzuki R, Sakata S, Hatano S, et al. RET, ROS1 and ALK fusions in lung cancer. Nat Med 2012;18:378–81.
27. Bergethon K, Shaw AT, Ou SH, Katayama R, Lovly CM, McDonald NT, et al. ROS1 rearrangements define a unique molecular class of lung cancers. J Clin Oncol 2012;30:863–70.
28. Davies KD, Le AT, Theodoro MF, Skokan MC, Aisner DL, Berge EM, et al. Identifying and targeting ROS1 gene fusions in non-small cell lung cancer. Clin Cancer Res 2012;18:4570–9.

Published OnlineFirst October 28, 2013; DOI: 10.1158/0008-5472.CAN-13-1103

Cancer Research
The Journal of Cancer Research (1916–1930) | The American Journal of Cancer (1931–1940)

AACR American Association for Cancer Research

MET and AXL Inhibitor NPS-1034 Exerts Efficacy against Lung Cancer Cells Resistant to EGFR Kinase Inhibitors Because of MET or AXL Activation

Jin Kyung Rho, Yun Jung Choi, Seon Ye Kim, et al.

Cancer Res 2014;74:253-262. Published OnlineFirst October 28, 2013.